Electrochemical Data Transferability within Li_yVOXO_4 (X = Si, $Ge_{0.5}Si_{0.5}$, Ge, $Si_{0.5}As_{0.5}$, $Si_{0.5}P_{0.5}$, As, P) Polyoxyanionic Compounds

M. E. Arroyo-de Dompablo,*,† P. Rozier,‡ M. Morcrette,§ and J-M. Tarascon§

Departamento de Química Inorgánica, Universidad Complutense de Madrid, 28040 Madrid, Spain, CEMES/CNRS, Groupe des Matériaux Inorganiques, BP 4347, 31055, Toulouse Cedex 4, France, and LRCS, Université de Picardie Jules-Verne, UMR 6007 CNRS, 33 rue Saint-Leu, 80039, Amiens, France

Received May 31, 2006. Revised Manuscript Received February 18, 2007

Given the interest of silicates as potential electrode materials for lithium batteries, it is critical to fully understand the role that the inductive effect of the polyoxyanionic group, $(XO_4)^{n-}$, plays on the electrochemical performance of polyoxyanionic compounds. In this work we have combined experiments and first-principles methods to investigate to which extent the inductive effect of the X−O bond within the XO_4^{n-} polyanion (X = Si, $Ge_{0.5}Si_{0.5}$, Ge, $Si_{0.5}As_{0.5}$, $Si_{0.5}P_{0.5}$, As, P) modifies the redox energy of the V^{5+}/V^{4+} couple in the Li_yVOXO_4 family of compounds. Calculations using the GGA+U method evidence a nice correlation between the X electronegativity (i.e., the magnitude of the XO_4 groups' inductive effect) and details of the crystalline and electronic structures of $Li_{y+1}V^{4+}OXO_4$/ $Li_yV^{5+}OXO_4$ phases such as bond distances or band gaps. Besides the inductive effect of the polyanionic group, we found that the chemistry of these 2D compounds is also correlated to the Li^+ site occupancy in the interlayer space. The calculated lithium insertion voltages display an almost linear dependence on the Mulliken X electronegativity; this offers promising prospects in the design of novel polyoxyanionic electrode materials. The new electrode materials Li_2VOGeO_4 and $Li_2VOSi_{0.5}Ge_{0.5}O_4$ have been electrochemically tested, providing good agreement between experimental and calculated lithium insertion voltages. Activation energies of the prepared compounds follow the band gap trend provided by the calculated data as well. Thus, experimental evidence support the computational results and the conclusions presented here.

Introduction

Understanding the factors governing the energy of the active redox couple of an electro-active material and, as a consequence, the working voltage of the lithium cell is of crucial importance in the design of innovative electrode materials. To illustrate this idea, one could consider, for instance, how the voltage developed by a lithium cell using the Fe^{3+}/Fe^{2+} couple depends on the specific material.[1] This redox couple is active at potentials ranging from 2.4 V in $Li_3Fe(MoO_4)_3$[2] to 2.5 V in $LiFeAs_2O_7$,[3] 3 V in $Fe_2(MoO_4)_3$,[4] 3.1 V in Li_2FeSiO_4,[5] 3.5 V in $LiFePO_4$,[6] and 3.6 V in $Fe_2(SO_4)_3$.[7] As stated by Goodenough's team, the energy of a given redox couple varies from one compound to another depending on two main factors: (1) the electrostatic field at the cation position and (2) the iono-covalency of the cation−anion bonding.[6,8,9] The relative importance of both factors can be properly studied on materials formed by MO_x polyhedra (M = transition metal cation) linked by tetrahedral polyatomic anions (XO_4^{n-} = PO_4^{3-}, AsO_4^{3-}, SO_4^{2-}, etc.). The electrostatic field follows the structure variations. On the other hand, the covalence of the M−O bond is different in isostructural compounds having different tetrahedral polyatomic anions due to the so-called inductive effect, which is a consequence of the different degree of covalence in the X−O bond. The meaning of inductive effect is "an experimentally observable effect of the transmission of charge through a chain of atoms by electrostatic induction" (*IUPAC Compendium of Chemical Terminology 2nd Edition*, 1997). However, while this concept looks simple and intuitive, it is desirable to quantitatively correlate the inductive effect of a polyatomic anion to the energy of the electrochemical reaction associated to a redox couple, and then to the voltage of a cell constructed with a given counter electrode. This issue gets even more relevance given the increasing interest in silicates as potential electrode materials; three silicates, Li_2FeSiO_4,[5,10] Li_2MnSiO_4,[10] and Li_2VOSiO_4,[11] have been proven to be electrochemically active to date. Therefore, there is not a lot known about the electrochemistry of silicates, in

* To whom correspondence should be addressed.
† Universidad Complutense de Madrid.
‡ CEMES/CNRS.
§ Université de Picardie Jules-Verne, UMR 6007 CNRS.

(1) Masquelier, C.; Patoux, S.; Wurm, C.; Morcrette, M. *Lithium Batteries: Science and Technology*; Kluwer Academic Publishers: Dordrecht, 2004.
(2) Alvarez-Vega, M.; Amador, U.; Arroyo-de Dompablo, M. E. *J. Electrochem. Soc.* **2005**, *152* (7), A1306.
(3) Masquelier, C.; Padhi, A. K.; Nanjundaswamy, K. S.; Goodenough, J. B. *J. Solid State Chem.* **1998**, *135*, 228.
(4) Manthiram A.; Goodenough, J. B. *J. Solid State Chem.* **1987**, *71*, 349.
(5) Nyten, A.; Abouimrane, A.; Armand, M.; Gustafsson, T.; Thomas, J. O. *Electrochem. Commun.* **2005**, *7* (2), 156.
(6) Padhi, A. K.; Nanjundaswamy, A. K.; Masquelier, C.; Okada, S.; Goodenough, J. B. *J. Electrochem. Soc.* **1997**, *144* (5), 1609.
(7) Manthiram, A.; Goodenough, J. B. *J. Power Sources* **1989**, *26*, 403.
(8) Padhi, A. K.; Nanjundaswamy, K. S.; Goodenough, J. B. *J. Electrochem. Soc.* **1997**, *144* (4), 1188.
(9) Padhi, A. K.; Nanjundaswamy, K. S.; Masquelier, C.; Goodenough, J. B. *J. Electrochem. Soc.* **1997**, *144* (8), 2581.

10.1021/cm0612696 CCC: $37.00
Published on Web 04/11/2007

contrast with the wide information acquired about the electrochemistry of phosphates during the past decade. In many cases the synthesis of lithium transition metal silicates is a very difficult task due to the thermodynamic instability of the desired phase during the synthesis. To minimize the experimental efforts, it would be desirable to correlate the well-known electrochemistry of phosphates to analogous silicates. We could question, for instance, which voltage difference can be expected between a phosphate and a silicate, if silicates are better electronic conductors than phosphates, and so forth. In this sense, we have recently investigated by first principles methods how the inductive effect of different polyoxyanions $(XO_4)^{n-}$ (X = Ge, Si, Sb, As, P) affects the lithium deintercalation voltage of olivine-$LiCo^{2+}XO4$, $Li_{y+1}V^{4+}OXO_4$, and $Li_yM^{2+}XO_4$ (M = Mn, Fe, Co, Ni within the structure of Li_2FeSiO_4) compounds.[12] In all cases the calculated lithium deintercalation voltage correlates to the Mulliken X electronegativity, displaying a linear dependence for each structural type/redox couple. In the present work, we combine first-principles and experimental methods to study in detail the correlations between properties for the $Li_{y+1}V^{4+}OXO_4$ family of compounds (X = Ge, Si, As, P, and their combinations) and the X electronegativity.

Solid-state chemists are quite familiar with the inductive effect based on simple ionic-covalence concepts and have used it sometimes as a sound platform to search for better electrode materials. The inductive effect is afterward the polarization of the V−O chemical bond caused by the polarization of the adjacent X−O bond. According to Pauling, the fractional ionic character of a A−B bond can be roughly estimated from the electronegativity difference of the bonding atoms A and B.[13] Furthermore, it is the bond polarity that governs the three types of bonds (covalent, metallic, and ionic) as demonstrated by visualizing the van Arkel-Ketelaar triangle, the vertices of which are labeled covalent, metallic, and ionic; the triangle is constructed quantitatively using the sum of the electronegativities of the constituents as a horizontal coordinate, and as a vertical axis its differences.[14−16] Following these elemental ideas, we postulated that in polyoxyanionic structures possessing M−O−X bonds the iono-covalent character of the M−O bonding is correlated to the electronegativity of X. It is well-documented that the evolution of band gaps, Fermi energies, or bond distances in binary solids correlates to the bond polarity or the electronegativity difference between the constituent elements.[16−19] Therefore, in polyoxyanionic compounds, bond lengths, band gaps, and lithium intercalation voltages might be related to the X electronegativity. In this work we will refer to the Mulliken electronegativity scale,[20,21] which defines the electronegativity as $\chi = (I + A)/2$, where I is the lowest first ionization potential of a ground-state free atom and A its corresponding electron affinity.

Vanadium-based oxides are well-known for presenting a wide range of structures mainly due to the versatility of the oxygenated surroundings adopted by vanadium ions in their +5 and +4 valence states. Among them the $Li_yVO(XO_4)$ family allows a comparison of the inductive effect of the polyanionic group $[XO_4]^{n-}$ on the redox potential of the V^{5+}/V^{4+} couple. The prototype structure Li_2VOSiO_4 (Figure 1a) was reported in the 1990s together with the existence of a solid solution $Li_2VO(Si_{1-x}Ge_xO_4)$.[22] This structure is built up with VO_5 square pyramids (SP) sharing corners with SiO_4 tetrahedra (Td) to form layers stacked along the *c*-axis and linked together by lithium ions located in distorted octahedra. The V^{4+} exhibits a typical short vanadyl V−O bond with the apical oxygen and four equivalent V−O distances with the equatorial oxygen ions. Prakash et al. showed that 0.7 lithium ions can be removed from Li_2VOSiO_4 compound at an average voltage of 3.63 V.[11] Studies reported in the phosphate vanadium based compounds show that among the different polymorphs the alpha-I form Li_yVOPO_4 ($y = 0, 1$) exhibits the Li_2VOSiO_4 structure type and is electrochemically active at 3.9 V.[23,24] In the arsenate family Li_yVOAsO_4 phase is reported to be present, even if not the most stable and easy to prepare form, a variety related to the alpha-I form structure type.[25] The combination of these different data allow one to define a $Li_yVO(XO_4)$ system with the same structure and the same active redox couple V^{5+}/V^{4+} while varying both the inductive effect of the polyanionic $[XO_4]^{n-}$ group (X = Si, $Si_{0.5}Ge_{0.5}$, Ge: $n = 4$ and X = P, As: $n = 3$) and the lithium amounts ($y = 1, 2$ for $n = 4$ and $y = 0, 1$ for $n = 3$). This family of compounds provides then an exceptional case to quantitatively analyze how the inductive effect of the different $(XO_4)^{n-}$ groups respectively shifts the redox potential of the V^{4+}/V^{5+} couple. For completeness, the electrochemistry of the $Li_2VOSi_{0.5}Ge_{0.5}O_4$ and Li_2VOGeO_4 compounds have been studied and reported in this paper and the study of the hypothetical compounds $Li_yVOSi_{0.5}As_{0.5}O_4$ and $Li_yVOSi_{0.5}P_{0.5}O_4$ aiming to extrapolate for $n = 3.5$ the results obtained for existing compounds (here $y = 0.5, 1.5$).

For sake of clarity the paper is organized following the lithium battery community's general way of thinking. In the Results and Discussion, section (a) deals with the lithium insertion voltage of $Li_yV^{5+}OXO_5$ compounds comprising the

(10) Dominko, R.; Bele, M.; Gaberscek, M.; Meden, A.; Remskar, M.; Jamnik, J. *Electrochem. Commun.* **2006**, *8* (2), 217.
(11) Prakash, A. S.; Rozier, P.; Dupont, L.; Vezin, H.; Sauvage, F.; Tarascon, J. M. *Chem. Mater.* **2006**, *18* (2), 407.
(12) Arroyo-de Dompablo, M. E.; Armand, M.; Tarascon, J.-M.; Amador, U. *Electrochem. Commun.* **2006**, *8* (8), 1292.
(13) Pauling, L. *The Nature of the Chemical Bond*; Cornell University Press: Ithaca, NY, 1960.
(14) van Arkel, A. *Molecules and Crystals in Inorganic Chemistry*; Wiley Interscience: New York, 1956.
(15) Ketelaar, J. A. A. *Chemical Constitution*; Elsewier: New York, 1958.
(16) Burdett, J. K. *Chemical bonding in solids*; Oxford University Press: Oxford, 1995.
(17) Campet, G.; Portier, J.; Subramanian, M. A. *Mater. Lett.* **2004**, *58* (3−4), 437.
(18) Nethercot, A. H. *Phys. Rev. Lett.* **1974**, *33* (18), 1088.
(19) Cox, P. A. *The electronic structure and chemistry of solids*; Oxford University Press: Oxford, 1987.
(20) Allen, L. C. *J. Am. Chem. Soc.* **1989**, *111* (25), 9003.
(21) Mulliken, R. S. *J. Chem. Phys.* **1934**, *2*, 782.
(22) Millet, P.; Satto, C. *Mater. Res. Bull.* **1998**, *33* (9), 1339.
(23) Kerr, T. A.; Gaubicher, J.; Nazar, L. F. *Electrochem. Solid State Lett.* **2000**, *3* (10), 460.
(24) Dupre, N.; Gaubicher, J.; Angenault, J.; Wallez, G.; Quarton, M. *J. Power Sources* **2001**, *97−8*, 532.
(25) Chernorukov, N. G.; Egorov, N. P.; Korshunov, I. A. *Zh. Neorg. Khim.* **1978**, *23* (10), 2672.

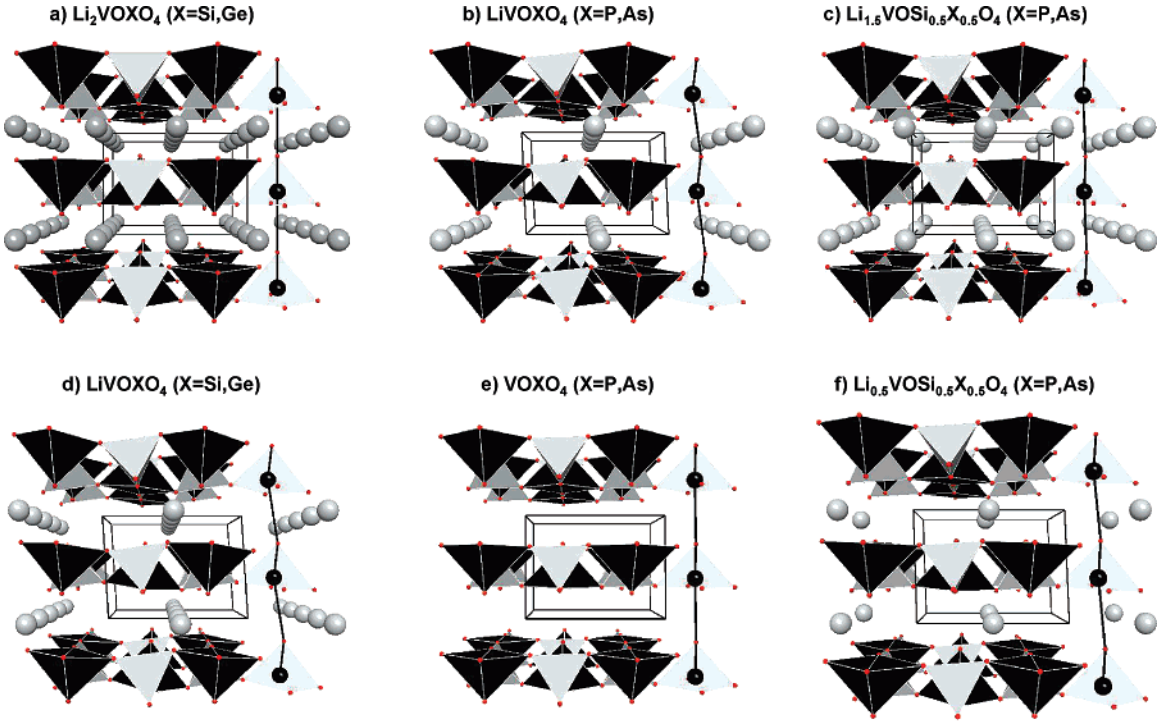

Figure 1. Crystal structures of Li_2VOSiO_4 (a), $LiVOPO_4$ (b), and $Li_{1.5}VOSi_{0.5}P_{0.5}O_4$ (c) and their corresponding delithiated phases $LiVOSiO_4$ (d), $VOPO_4$ (e), and $Li_{0.5}VOSi_{0.5}P_{0.5}O_4$ (f). Atomic position are taken from the computational results after fully relaxing the structures (optimized structures).

experimental results followed by first-principles predictions. In section (b) we address the crystalline structures of lithiated and delithiated materials including a comparison between calculations and experiments whenever experimental data are available. Section (c) presents the experimental determination of activation energies and the analysis of the calculated electronic structures. This outline was done according to relevant aspects that should be considered in the search for promising electrode materials, starting with the common objective of each battery researcher that is to have the appropriate tools to tentatively design a new high lithium insertion voltage compound (section (a)). A good electrode should also display a nicely reversible lithium insertion process to favor long-term cyclability, and this is intimately linked to the crystalline structure (section (b)). Finally, it is very important to anticipate the polarization of the positive electrode since it directly governs its power rate capability that depends on the intrinsic electrical conductivity of the active material. While computing the total energy of a compound does not provide any information about the Li mobility, information on the *intrinsic* electronic conductivity can be inferred from the electronic structure (section (c)).

Methodology

Experimental. The Li_2VOSiO_4, Li_2VOGeO_4, and $Li_2VOSi_{0.5}Ge_{0.5}O_4$ phases reported herein were prepared by a ceramic route (Millet and Satto[22]). Stoichiometric amounts of Li_2SiO_3 (Aldrich) and Li_2GeO_3 (Aldrich) and homemade VO_2 were thoroughly mixed, pressed into 12 × 4 mm pellets, wrapped within a platinum foil (to avoid direct contact of the reaction mixture with the silica tube), and then placed in a fused silica ampule that was then evacuated and sealed. The ampule was heated at a rate of 4 °C/min to 925 °C for 48 h and then cooled to room temperature by turning the furnace off. The resulting red brownish pellets were powdered prior to characterizing the structural aspects. The powders were single-phased, as deduced from their X-ray diffraction pattern recorded on a Scintag diffractometer (Cu Kα radiation $\lambda = 1.5418$ Å). The refined cell parameters fall in good agreement with previously reported literature values (Table 1).[22] The electrochemical reactivity of both lithiated and delithiated phases vs Li was tested using laboratory Swagelok cells. The as-made lithiated samples being barely electrochemically active were mixed with 20% (by weight) carbon and ball-milled for 10 h in a Fritch apparatus. Swagelok-type cells were assembled in an argon-filled glovebox with about 10 mg of the ball-milled mixture and separated from the negative electrode (lithium foil) by two sheets of fiber glass disks, the whole being soaked with a $LiPF_6$ (1 M) solution in ethylene carbonate (EC)/dimethyl carbonate (DMC) mixture (1/1 v/v). Galvanostatic tests were conducted with a Mac Pile controller at constant temperature of 25 °C. For ac electrical conductivity measurements, the lithiated powders were first pressed into pellets by means of uni-axial pressure (500 kg cm^{-2}). The resulting pellets were sintered under N_2 at 900 °C for 24 h, resulting in ∼76% dense pellets. Careful control and polishing of the pellet surfaces was ensured before platinum deposition (sputtering) on opposite faces of the pellets. ac impedance measurements were done in air over the 403−518 K temperature range using an Autolab PGSTAT20 impedance analyzer by applying 350 mV amplitude in a frequency range of 1 MHz to 1 Hz.

Computational. A good description of the DFT method and its application to the study of lithium battery materials can be found in refs 26 and 27. In this work, we have performed total energy calculations based on DFT in the Generalized Gradient Approximation with the Hubbard parameter correction (GGA+U) following the rotationally invariant form as implemented in VASP.[28−30] Within this approach, two correction terms enter as independent parameters

(26) Aydinol, M. K.; Kohan, A. F.; Ceder, G.; Cho, K.; Joannopoulos, J. *Phys. Rev. B* **1997**, *56* (3), 1354.
(27) Zhou, F.; Cococcioni, M.; Marianetti, C. A.; Morgan, D.; Ceder, G. *Phys. Rev. B* **2004**, *15*, 235121-1.
(28) Kresse, G.; Furthmuller, J. *Comput. Mater. Sci.* **1996**, *15*, 6.

Table 1. Cell Parameters (in Angstroms) for the Optimized Structures of $Li_{y+1}V^{4+}XO_5$ and $Li_yV^{5+}XO_5$ Compounds (Set II)[a]

lattice parameters	Ge $r = 0.67$	$Ge_{0.5}Si_{0.5}$	Si $r = 0.54$	$Si_{0.5}As_{0.5}$	$Si_{0.5}P_{0.5}$	As $r = 0.60$	P $r = 0.52$
			V^{4+}				
a	6.632 (6.487^{22})	6.527 (6.436^{22})	6.434 (6.368^{22})	6.512	6.404	6.583	6.345 (6.279^{47})
b	6.632 (6.487)	6.527 (6.436)	6.434 (6.368)	6.512	6.404	6.618	6.382 (6.279)
c	4.590 (4.517)	4.583 (4.493)	4.530 (4.449)	4.627	4.575	4.679	4.592 (4.442)
α, β, γ	90, 90, 90	90, 90, 90	90, 90, 90	89.4, 89.4, 90.1	89.3, 89.3, 90.5	87.4, 90, 90	87.3, 90, 90
volume	201.91 (190.08)	194.93 (186.11)	187.57 (180.4)	196.23	187.63	203.67	185.77 (175.2)
			V^{5+}				
a	6.456	6.350	6.264(6.206^{11})	6.398	6.291	6.473	6.248 (6.014^{56})
b	6.610	6.500	6.397 (6.206)	6.400	6.291	6.486	6.255 (6.014)
c	4.816	4.782	4.717 (4.572)	4.817	4.734	4.714	4.600 (4.434)
α, β, γ	85.9, 90, 90	85.8, 90, 90	86.3, 90, 90	87.28, 92.8, 89.6	87.5, 92.6, 89.9	90, 90, 90	90, 90, 90
volume	205.05	196.89	188.63 (176.08)	196.79	187.13	197.97	179.81 (160.37)
$c.\sin\alpha$	4.803	4.769	4.707	4.811	4.729		

[a] Ionic radii from Shannon-Prewitt (Å).[55] Experimental values in parentheses.

in the calculation method: the onsite Coulomb correlation term *U*, and the *J* term, which is an approximation to the Stoner exchange parameter.[31] The *U* and *J* correction basically give an additional contribution from a Coulomb interaction (pairs with antiparallel spins) and exchange interactions (pairs with parallel spins) to those orbitals that keep their "atomlike" (e.g., localized) behavior and thus correct their energies.[32,33] *U* and *J* can be extracted from self-consistent calculations.[27] An alternative route consists of selecting these values so as to account for the experimental results whatever they are: equilibrium volume, magnetic moment, band gap, structure, or lithium insertion voltage as in the present work.[34] We have in the present case computed the total energies of Li_2VOSiO_4 and $LiVOSiO_4$ within the GGA+U approximation with *U* values ranging from 0 to 5 eV and with *J* being equal to either 0 or 1 eV. Thereafter, we set $U = 4$ eV and $J = 1$ eV to calculate the total energy of all other $Li_{y+1}V^{4+}XO_5$ and $Li_yV^{5+}XO_5$ compounds. In the case of V^{5+}-based compounds the total energy was also calculated within the pure GGA, i.e., without introducing the *U* and *J* correction terms. For the exchange and correlation functional we chose a form suggested by Perdew, Burke, and Ernzerhof (PBE).[35] A number of one, five, four/five, and six valence electrons are taken into account for each Li, V, Si(Ge)/P(As), and O atom, while the remaining core electrons together with the nuclei are described by pseudo-potentials following the Projector Augmented Wave (PAW) method.[36] To evaluate the influence of the basis set on the overall results, a second set of calculations was performed using the PBE potentials but increasing the number of valence electrons to 3 and 11 for Li ($1s^22s^1$) and V ($3p^64s^2d^3$), respectively. We will refer to this set of calculations as "set II", while the one with less valence electrons will be denoted as "set I". Hence, it is important to stress that different pseudo-potentials have been used in set I and set II; in the latter, smaller core pseudo-potentials have been introduced to explicitly introduce the semi-core states into the calculations. Introducing the semi-core states of V 3p and Li 1s as valence states in the calculation (set II) provides more accurate results, though it comes at the expense of a high price in computational power. The wave functions were expanded on a plane-wave basis set with kinetic energy below 500 eV. The integration in the Brillouin zone is done by using the tetrahedron method corrected by Blöchl on a set of *k*-points ($4 \times 4 \times 6$) determined by the Monkhorts-Pack scheme (48 irreducible *k*-points). A convergence of the total energy close to 5 meV per formula unit is achieved with such parameters. The initial cell parameters and atomic positions of Li_2VOSiO_4 were taken from Millet and Satto,[22] with the unit cell containing two formula units ($Li_4V_2Si_2O_{10}$). Thereafter, compositional variations were introduced placing different X atoms (X = P, As, Ge) in the Si positions to form $Li_yV^{4+}OXO_4$ ($y = 1$: X = P, As, $y = 1.5$: X = $P_{0.5}Si_{0.5}$, $As_{0.5}Si_{0.5}$ and $y = 2$: X = Ge, $Si_{0.5}Ge_{0.5}$). Notice that for the mixed compounds one Si atom is replaced by Ge, Si, or P ($Li_4V_2SiXO_{10}$). In all cases a ferromagnetic configuration was used to define the initial ground state of $Li_yV^{4+}OXO_5$ and the calculations were done considering the spin polarization. All the lithiated structures were fully relaxed (cell parameters, atomic positions, and cell shape); Li ions were selectively removed from these optimized structures, leading to $Li_yV^{5+}OXO_4$ ($y = 0$: X = P, As, $y = 0.5$: X = $P_{0.5}Si_{0.5}$, $As_{0.5}Si_{0.5}$ and $y = 1$: X = Ge, $Si_{0.5}Ge_{0.5}$) compounds, the structures of which were also fully relaxed. The final energies of the optimized geometries were recalculated so as to correct the changes in the basis set of wave functions during relaxation. Preparation and analysis of VASP files were done primarily with the CONVASP code.[37]

Results and Discussion

(a) Lithium Insertion Voltages. Swagelok LiVOSi(Ge)-O_4/Li cells were assembled and cycled in a galvanostatic mode between 2.5 and 4 V with a discharge and charge current of 10 μA/cm^2. The voltage composition curves collected for the three cells show a plateau, indicative of a two-phase intercalation process. For reasons of length and clarity, we reported only on the derivative curves (d*x*/d*V* vs *V*) that are more appropriate for accurately determining redox potential values (Figure 2). Note that the redox potential, initially of 3.63 V vs Li^+/Li^0 for the Li_2VOSiO_4 phase, decreases to about 3.55 V for the Li_2VOGeO_4 phase and takes an intermediate value of 3.58 V for the 50/50 Ge/Si phase. However, such relation between potential and inductive effect does not come as a surprise since it was already spotted and described by Goodenough et al. for the phos-

(29) Liechtenstein, A. I.; Anisimov, V. I.; Zaanen, J. *Phys. Rev. B* **1995**, *52* (8), R5467.
(30) Kresse, G.; Furthmuller, J. *Phys. Rev. B* **1996**, *54*, 169.
(31) Anisimov, V. I.; Zaanen, J.; Andersen, O. K. *Phys. Rev. B* **1991**, *44* (3), 943.
(32) Anisimov, V. I.; Solovyev, I. V.; Korotin, M. A.; Czyzyk, M. T.; Sawatzky, G. A. *Phys. Rev. B* **1993**, *48* (23), 16929.
(33) Bengone, O.; Alouani, M.; Blochl, P.; Hugel, J. *Phys. Rev. B* **2000**, *62* (24), 16392.
(34) Zhou, F.; Cococcioni, M.; Kang, K.; Ceder, G. *Electrochem. Commun.* **2004**, *6* (11), 1144.
(35) Perdew, J. P.; Burke, K.; Ernzerhof, M. *Phys. Rev. Lett.* **1996**, *77* (18), 3865.
(36) Bloch, P. E. *Phys. Rev. B* **1994**, *50*, 17953.
(37) Morgan, D.; Curtarolo, S.; Ceder, G. http://burgaz.mit.edu/PUBLICATIONS/codes.php.

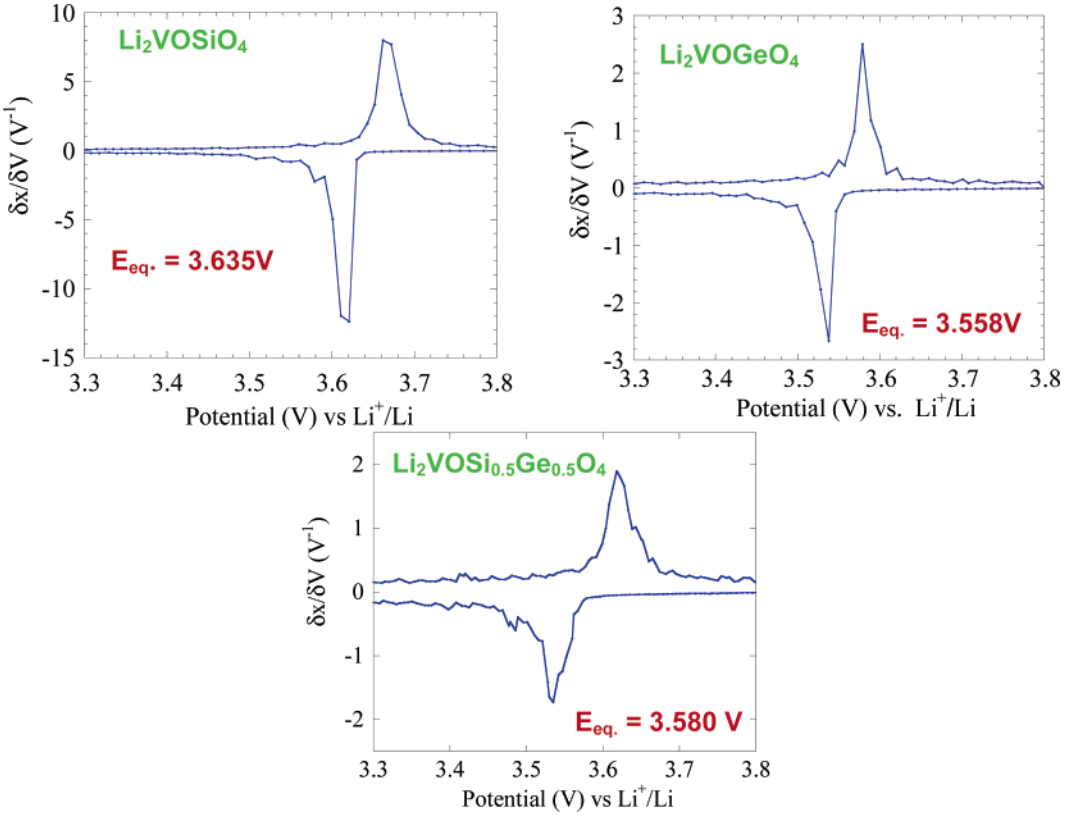

Figure 2. Differential capacity plots ($\delta x/\delta V$) for $Li_2VO(Si/Ge)O_4$ materials.

phates. More covalent X−O bonds will make the V−O bonds less covalent through the inductive effect, resulting in a lowering of the antibonding states (e.g., energy of the V^{5+}/V^{4+} redox couple), and leading to a higher lithium insertion voltage. Thereby it is possible, with polyoxyanionic structures possessing M−O−X bonds, to act on the nature of X to change the iono-covalent character of the M−O bonding through the inductive effect of the counteranion, to establish a systematic mapping and tuning of transition-metal redox potentials. For instance, with the use of the phosphate polyanions PO_4^{3-}, the Fe^{3+}/Fe^{2+} and V^{4+}/V^{3+} redox couples lie at higher potentials than when in the oxide form.[1] However, a quantification of the voltage shift due to the inductive effect of the polyanion group is experimentally very costly. Goodenough and co-workers showed that a change from sulfate to phosphate ions lowers the open-circuit voltage of isostructural compounds in 0.8 V.[9] Such a result comes from the study of at least four compounds ($Li_{3+x}M_2(PO_4)_3$, $Li_xM_2(SO_4)_3$ with M = Fe, V) comprising the preparation, structural characterization, and electrochemical testing.[9] Obviously, applying computational methods to precise voltage shifts would minimize experimental efforts.

Since 1997,[26] density functional theory (DFT) has been widely used to predict the average voltage of lithium insertion in many compounds. Assuming that the changes in volume and entropy associated with the intercalation are negligibly small, the voltage can be extracted from the calculated total energies.[26] In systems with high electron−electron repulsion, introducing a *U*-parameter correction term into the density functional theory improves the accuracy in the prediction of lithium insertion voltage, lowering the differences with experimental voltages to the range of a few meV.[27,34,38−40] In the Li_yVOXO_4 family vanadium ions are well separated by SiO_4 tetrahedra, preventing any 3d orbital from overlapping, and therefore a *U* correction term must be included in the calculation to account for these highly localized electrons. As recently demonstrated by Wang et al.,[41] the incapability of the pure DFT to accurately predict redox energies is a common feature to any redox reaction where the electron is transferred between very distinct environments (e.g., metallic state in lithium to localized 3d orbital in Li_yVOSiO_4); hence, the DFT+U method improves the accuracy on the prediction of such redox potentials even if the compound accepting the electron has a transition metal ion with a d^0 configuration (as V^{5+}, or Cr^{6+}-based compounds). Figure 3a shows the calculated lithium insertion voltage for the $LiVOSiO_4 \leftrightarrow Li_2VOSiO_4$ electrochemical reaction plotted as a function of several *U* and *J* parameter values (see Methodology section); the experimental voltage is indicated by a horizontal line. The calculated voltage steeply increases with the value of the *U* parameter, as previously reported for olivine-$LiFePO_4$,[42] olivine-$LiCoXO_4$ (X = P, As),[43] and Li_2FeSiO_4.[12] Without the *U* correction term the insertion voltage is underestimated by ca. 1 V, whereas for *U* values greater than 4 eV the voltage is overestimated. For the set I of calculations the most accurate estimation of the experimental voltage is being reached at $U = 4$ eV and $J = 1$ eV. Although for the

(38) Le Bacq, O.; Pasturel, A.; Bengone, O. *Phys. Rev. B* **2004**, *69* (24), 245107.
(39) Arroyo-de Dompablo, M. E. A.; Gallardo-Amores, J. M.; Amador, U. *Electrochem. Solid State Lett.* **2005**, *8* (11), A564.
(40) Zhou, F.; Marianetti, C. A.; Cococcioni, M.; Morgan, D.; Ceder, G. *Phys. Rev. B* **2004**, *69*, 201101(R).
(41) Wang, L.; Maxisch, T.; Ceder, G. *Phys. Rev. B* **2006**, *73*, 195107-1.
(42) Zhou, F.; Marianetti, C. A.; Cococcioni, M.; Morgan, D.; Ceder, G. *Phys. Rev. B* **2004**, *69* (20), 201101.
(43) Arroyo-de Dompablo, M. E.; Amador, U.; Garcia-Alvarado, F. *J. Electrochem. Soc.* **2006**, *153* (4), A673.

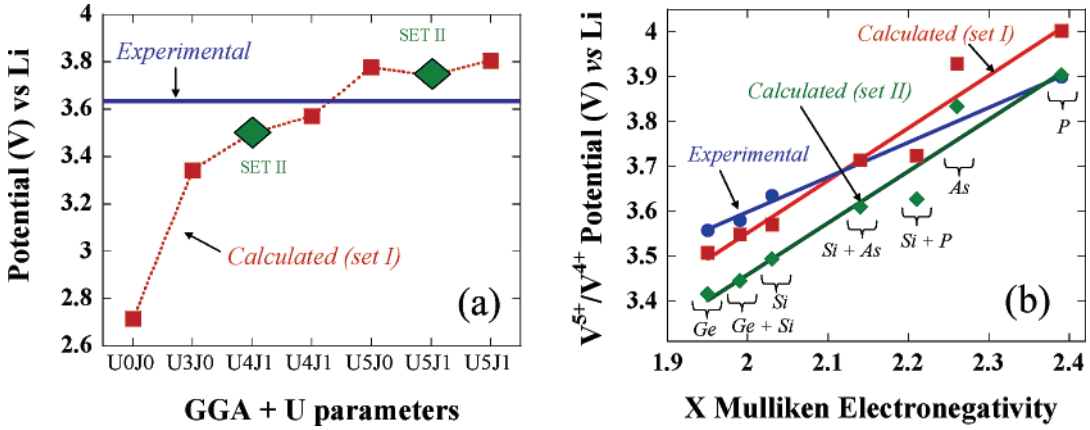

Figure 3. (a) Calculated lithium insertion voltage for Li_yVOSiO_4 as a function of the *U* and *J* parameters used in the GGA+U method. The experimental voltage of Li_2VOSiO_4 is indicated by a horizontal line. Green diamonds denote the calculated data obtained using the set II of potentials which include the V 3p and Li 1s states as valence states. (b) Calculated lithium insertion voltage for the $Li_yV^{5+}OXO_4$ compounds (X = Ge, Si, $Si_{0.5}As_{0.5}$, $Si_{0.5}P_{0.5}$, As, P) vs the Mulliken X electronegativity (in Pauling units). Experimental values together with the corresponding linear fit are given for comparison.

set II of potentials (green diamonds in Figure 3a) a more accurate estimation of the experimental voltage would require a slightly larger *U* value, aiming to compare the results from set I and set II, we selected $U = 4$ eV and $J = 1$ eV for the remaining calculations. For nomenclature consistency with previous works, thereafter we will refer to the $U_{effective}$ value (denoted simply as *U*), being $U_{effective} = U - J$, i.e., 3 eV. Special care is certainly needed to select a correct *U* value since *U* should have a physical meaning and should be in a correct range of value. $U = 3$ eV falls in the range found in other V^{4+} or V^{5+} compounds: 3.1 eV in VO/V_2O_5,[41] 2.72 eV in $MV_nO_{(2n+1)}$,[44] 3.2−4.2 eV in $K_6[V_{15}As_6O_{42}(H_2O)]\cdot 8H_2O$,[45] or 5.9 eV in VO.[31] Regarding the physical meaning, depending on the *U* value that is chosen, the calculated electronic band gap will be affected, as we will discuss in section (c).

Figure 3b plots the calculated and experimental lithium insertion voltage for $Li_yV^{5+}OXO_4$ (X = P, As, $P_{0.5}Si_{0.5}$, $As_{0.5}Si_{0.5}$, Si, Ge) compounds as a function of the Mulliken electronegativity of the central atom X (in Pauling units) of each polyoxyanionic group (XO_4). Independent of the number of valence electrons included in the calculation (set I or set II), the calculated voltage increases with the X electronegativity displaying an almost linear dependence. The experimental voltages of lithium insertion into $LiVOSiO_4$, $LiVOGe_{0.5}Si_{0.5}O_4$, $LiVOGeO_4$, and $VOPO_4$[23] well agree with the calculated values, supporting the computational results. Moreover, experimental data also provide a linear voltage = f(χ) relationship. Therefore, it is possible to extrapolate the insertion voltage of any other $Li_yV^{5+}(X'X''X'''...)_1O_5$ compound belonging to this family. For instance, for X = V^{5+} ($\chi = 1.63$) the calculated and experimental linear fittings of Figure 3b give voltages of 3.1 and 3.3 V, respectively. These values of the hypothetical $VOVO_4$ are comparable to the V^{4+}/V^{5+} redox potential value of 3.4 V in V_2O_5.[46]

We have so far demonstrated that the experimental/computational lithium insertion voltages of the $Li_yV^{5+}OXO_4$ family of compounds can be correlated to values of tabulated Mulliken electronegativities. A linear correlation is observed in all cases, even when the set I of potentials is used (less accurate calculation, but faster).

(b) Crystal Structure. Lithium sites are fully occupied in Li_2VOSiO_4, and oxidizing this compound would lead to a 50% Li site occupancy in $LiVOSiO_4$. It is difficult to simulate the $LiVOXO_4$ structure using periodic electronic structure methods unless a lithium/vacancy order is imposed to the cell used in the calculations. As there is no experimental evidence of any Li ordering in the experimentally prepared $Li_{1.18}VOSiO_4$,[11] or in the isostructural $LiVOPO_4$,[47] we set up different Li-ordering models by selectively removing lithium ions from the relaxed structure of Li_2VOSiO_4. In a first model, the oxidation corresponds to removing all the lithium in one over two rows. The tetragonal symmetry of the starting compound does not allow to choose between the [100] or [010] direction but of course does drive, in the resulting oxidized sample, to differentiate them. Considering the lithium chains running for example along the [100] direction in the starting material, removing all the lithium in one over two rows leads to formation along [010] alternate fully occupied and empty rows (as shown in Figure 1). We calculated the energy of a second model, where lithium ions are evenly removed along both [010] and [100] directions, so as to keep the tetragonal symmetry of Li_2VOSiO_4. This latter configuration resulted in lower stability than the one shown in Figure 1d, with energy differences of 0.157 and 0.062 eV/f.u. for $LiVOSiO_4$ and $LiVOPO_4$, respectively. We should recall that DFT methods provide information for structures at 0 K (no entropy term is accounted for). At higher temperatures the configurational entropy term might be large enough to generate a random lithium distribution.

Table 1 summarizes the calculated lattice parameters of V^{4+} and V^{5+} Li_yVOXO_4-type compounds obtained after fully relaxing the structures. Experimental values are given in parentheses; generally speaking, a good agreement is observed with differences below 5%. However, the prepared "$Li_{1.18}VOSiO_4$" and $LiVOPO_4$ possess a tetragonal symmetry,[11,47] which is not reproduced by the computational method. As demonstrated below, the calculated orthorombic

(44) Korotin, M. A.; Elfimov, I. S.; Anisimov, V. I.; Troyer, M.; Khomskii, D. I. *Phys. Rev. Lett.* **1999**, *83* (7), 1387.
(45) Boukhvalov D. W.; Dobrovitski V. V.; Katsnelson M. I.; Lichtenstein A. I.; Harmon, B. N.; Kogerler, P. *J. Appl. Phys.* **2003**, *93* (10), 7080.
(46) Delmas, C.; Cognacauradou, H.; Cocciantelli, J. M.; Menetrier, M.; Doumerc, J. P. *Solid State Ionics* **1994**, *69* (3−4), 257.

symmetry responds to the order of lithium ions imposed in the calculated unit cell. The characterization of $LiVOPO_4$ by means of neutron and X-ray diffraction reveals that Li ions are randomly distributed over $^1/_4$ of the 8j sites of the structure.[47] Since there are no experimental data at low temperature, one cannot discard that Li ions would order below room temperature, resulting in a lowering of the tetragonal symmetry. Preparation of $LiVOSiO_4$ was attempted by chemical delithiation of Li_2VOSiO_4.[11] The XRDP matching of the delithiated sample was achieved when considering the sample to be a mixture of the starting Li_2VOSiO_4 compound and the Li_xVOSiO_4 delithiated compound. The compositional analysis of the Li_xVOSiO_4 phase revealed its composition to be $Li_{1.18}VOSiO_4$. Though the poor quality of the XRD data did not allow the refinement of the atomic position of the ions in the cell, no superstructure reflections attributable to lithium ordering were observed. In the prepared $Li_{1.18}$ $VOSiO_4$, the departure from the ideal stoichiometry, $LiVOSiO_4$, would also contribute to the prevention of lithium ordering.

As expected, for each oxidation state the volume tends to increase with the size of X (Table 1). Delithiation causes a minor effect over the volume of the unit cell, the exception made of X = As, P, where lithium ions are completely removed from the structure so that the delithiated form consists of neutral $[VXO_5]$ layers. Noteworthy, the calculated lattice parameters of Li_2VOSiO_4 within the GGA+U, as a function of the *U* value, display a small variation (1%), stressing that experimental redox voltages are more appropriate for meaningfully defining *U*. In both V^{4+} and V^{5+} series of compounds the *a* and *b* parameters display a slight tendency to increase with the size of X. Lithium de-insertion produces the shrinkage within the $[VOXO_4]^{n-}$ layers due to the oxidation of V^{4+} into the smaller V^{5+}. The interlayer distance corresponds to *c* sin α and is added for comparison in Table 1 for compounds presenting α different from 90°. At this point we should analyze two aspects in these structures: (i) the amount of lithium ions in the interlayer space and (ii) the structural distortions from the tetragonal symmetry of Li_2VOSiO_4. Both factors are strongly correlated as deduced from Figure 1. In the silicate and germanate Li_2VOXO_4 (Figure 1a) the Li sites are fully occupied, and owing to this full occupancy, each oxygen of the V^{4+} square pyramid also belongs to the Li^+ and Si^{4+} polyhedra, resulting in four equivalent V−O distances and a tetragonal symmetry (see V−O distances in Table 2). As commented above, in our model, the oxidation of such compounds leads to alternate fully occupied and empty rows of Li along [010]. This arrangement induces a puckering of the layer along the *b* direction which becomes longer than the *a* one. The evolution of the V−O distances (Table 2) shows that V^{5+} adopts its typical surrounding in the form of a distorted SP, the V^{5+} cation moving toward a tetrahedron coordination (four short distances at about 1.8 and a longer one close to 2.0). The reduced $LiVOXO_4$ compounds with X = As or P correspond to the same lithium amount (50% occupancy of the lithium sites) but with V in the +4 valence state. Here again a puckering of the layer is observed but the deformation

Table 2. V−O Bond Lengths (in Å) for the Optimized Structures of $Li_{y+1}V^{4+}OXO_4$ and $Li_yV^{5+}OXO_4$ Compounds (Set II); Angle Corresponds to the (Long V−O)−V−(Short V−O) Angle (Experimental data are given in parenthesis)[a]

distances (Å)	Ge		Si		$Ge_{0.5}Si_{0.5}$		$Si_{0.5}As_{0.5}$		$Si_{0.5}P_{0.5}$		As		P	
		e.s.d. (×10⁴)		e.s.d. (×10⁴)		e.s.d. (×10⁴)		e.s.d. (×10⁴)		e.s.d. (×10⁴)		e.s.d. (×10⁴)		e.s.d. (×10⁴)
V^{4+}−O	1.668 (1.621)		1.671 (1.629)		1.669 (1.631)		1.659		1.656		1.643		1.643 (1.582)	
	1.995 × 4 (1.952 × 4)		1.989 × 4 (1.959 × 4)		1.970 × 2 (1.955 × 4)		1.958	4.96	1.935	8.99	1.965	5.82	1.954 (1.95 × 44)	7.55
					2.017 × 2		1.991	0.37	1.998	0.02	2.007	0.13	2.003	0.09
							2.028	1.56	2.010	0.55	2.007	0.13	2.003	0.09
							2.034	2.49	2.065	10	2.077	9.82	2.077	10
average basal	1.995		1.989		1.993		2.003		1.995		2.014		2.009	
distortion	0		0		0.00013		0.00024		0.00050		0.00040		0.00048	
O−V−O angle	180 (180)		180 (180)		180 (180)		170.82		171.44		164.80		165.35 (180)	
		e.s.d. (×10⁴)		**e.s.d. (×10⁴)**		**e.s.d. (×10⁴)**		**e.s.d. (×10⁴)**		**e.s.d. (×10⁴)**		**e.s.d. (×10⁴)**		**e.s.d. (×10⁴)**
V^{5+}−O	1.646		1.644		1.646		1.629		1.627		1.613		1.611 (1.578)	
	1.808	30	1.809	30	1.808	30	1.831	20	1.823	20	1.915	0.03	1.913 (1.858 × 4)	0.02
	1.886	1.7	1.882	1.6	1.884	2.0	1.893	0.91	1.900	0.40	1.918	0.002	1.916	0.0002
	1.886	1.7	1.882	1.6	1.884	2.0	1.940	2.34	1.906	0.09	1.918	0.0009	1.916	0.0002
	2.065	60	2.051	60	2.066	70	1.976	10	2.018	30	1.924	0.05	1.919	0.04
average basal	1.911		1.906		1.910		1.910		1.912		1.919		1.916	
distortion	0.0024		0.0022		0.0025		0.0008		0.0013		0.0000 022		0.0000 015	
O−V−O angle	161.35		163.28		161.07		165.99		167.79		178.36		178.77 (180)	

[a] Distortion: $\Delta = 1/N \sum n = 1,N \{(dn - \langle d_{basal}\rangle)/\langle d_{basal}\rangle\}^2$. esd: $\{(dn - \langle d_{basal}\rangle)/\langle d_{basal}\rangle\}^2$; d_{basal} = average basal.

(47) Dupre, N.; Wallez, G.; Gaubicher, J.; Quarton, M. *J. Solid State Chem.* **2004**, *177* (8), 2896.

is smaller than that in silicate or germanate. The distribution of V−O distances shows clearly that the vanadyl bond is still present and that V^{4+} does not move toward the tetrahedron coordination. Oxidation of these latter compounds leads to complete removal of the lithium, leading to free interlayer space. The $VO(P,As)O_4$ structure recovers the tetragonal symmetry. Strangely, the distribution of the V−O distances is not in agreement with the one typically obtained for V^{4+} and V^{5+} oxygenated environment. Even if the diminution of the volume of the SP is observed during the oxidation, the distribution of the V−O distances shows a higher distortion in the V^{4+} case than in the V^{5+} one. This unusual distortion can be related to the fact that the V^{4+} valence state is associated with the presence of Li^+ in the interlayer space, inducing the sharing of oxygen ions.

Since Li ions do not order (at room temperature) in the prepared $LiVOXO_4$ compounds, it is important to confirm that the structural distortion is due to the ordering of lithium ions between the layers. With this aim we simulated the relaxed structure of hypothetical compounds obtained using a mixture of Si and P or As in the Td environment together with V in +5 or +4 valence state, allowing simulation of the relaxed structure for other lithium occupancy $Li_{1.5}V^{4+}O(Si_{0.5}X_{0.5})O_4$ and $Li_{0.5}V^{5+}O(Si_{0.5}X_{0.5})O_4$. Lithium ions are removed one site over two along one chain over two from the fully occupied case to reach the 75% occupancy (V^{4+} compound) and one site over two along the [100] remaining chains of the $LiVOSiO_4$ structure type to reach the 25% occupancy (V^{5+} compound). In both cases that drives the structural distortions associated here again to a puckering of the layers. Note that the ordered occupancy along the second direction ([100] using our choice) leads to the distortion of the layers along the corresponding cell parameter (*a* using our choice) and the departure of the corresponding angle which becomes different from 90°. The distribution of the V−O distances is in agreement with the usual ones for both V^{4+} and V^{5+} environments, the latter exhibiting the tetrahedral distortion. Then clearly one can say that the lithium location is responsible for the structural distortion. A full or empty occupancy leads to symmetric structure while partial occupancies lead to structural distortion. The puckering of the layer appears in the direction where there is alternatively lithium and vacancies (along only one direction for 50% occupancy corresponding to alternate empty and full lithium rows and along both directions for 75% and 25% occupancy obtained when lithium and vacancies alternate in both directions). Interestingly apart for empty lithium free compounds, whatever the structure symmetry, the distribution of V−O distances is in agreement with the V valence state.

Next, it is important to clarify whether this structural distortion is somehow related to the inductive effect of the polyoxyanionic group (X electronegativity). Based on the observation that the major distortion affects the α angle, we chose as rough criteria to describe the structural distortion of the O−V−O angle formed between V ions, the vanadyl bond, and the V−O bond opposite to it. As shown in the inset of Figure 4, this angle is 180° in the tetragonal symmetry (see Figure 1 and Table 2). The departure from 180° of this angle is represented in Figure 4 as a function of the Li site occupancy for set II of the calculations (set I gives equivalent results with departure-angle values ranging from

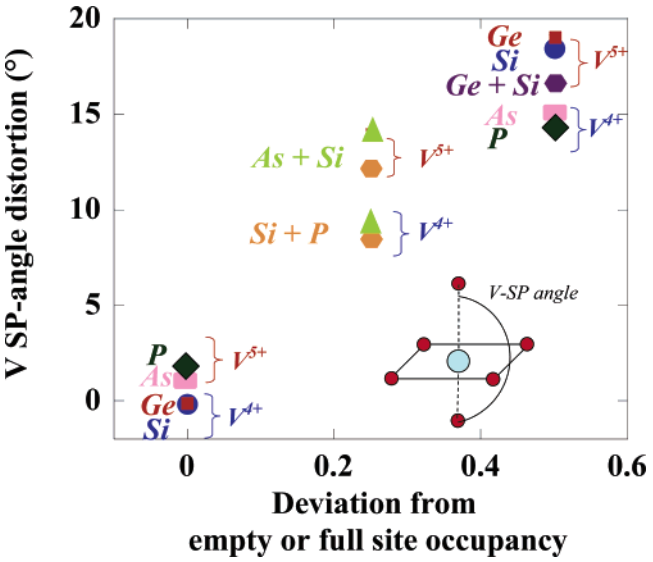

Figure 4. V square pyramid (SP) distortion in $Li_yV^{5+}OXO_4$ and $Li_{1+y}V^{4+}OXO_4$ versus the lithium site occupancy (set II of calculations). The distortion is defined as the departure from 180 of the O═V−O angle, where V═O refers to the vanadyl bond and V−O to its opposite bond along the *c*-axis of the tetragonal structure, as graphically described in the inset.

0 to 15°). It can be inferred that the structural distortion from the tetragonal symmetry is due to the different Li sites occupancy and independent of the inductive effect of the polyoxyanionic group.

Figure 5 shows the evolution of the calculated average V−O(basal) distances in V^{4+} (Figure 5a) and V^{5+} (Figure 5b) compounds versus the electronegativity of the central atom X of each polyoxyanionic group (XO_4) (set I in red, set II in green). Looking for general trends, the lines connect elements from the same period (period 3: Si, P and period 4: Ge, As). In both V^{4+} and V^{5+} series of compounds, the general trend is that the average V−O(basal) distance increases with X electronegativity, i.e., the inductive effect magnitude of the XO_4 group. Higher electronegative X elements polarize more the oxygen electron density, resulting in a more polarized (ionic) V−O bond. This is nicely observed moving along a period (Si−P, Ge−As) where the X−O bond progressively acquires a stronger covalent character, rendering the V−O bond more ionic in character. Regardless of this general trend, a clear splitting is observed between the elements of the $n = 3$ (Si, P) and $n = 4$ (Ge, As) periods. Going down a column, we are moving to 4d orbitals that are more expanded owing to a modification of the screening effect (Slater coefficients) together with the appearance of the f levels with, as the bottom line, the effective nuclear charge increasing. Interestingly, according to the Allred-Rochow electronegativity scale [$(\chi_A = 0.359Z_A/r_A^2 + 0.744)$, where Z_A, as determined by the Slater rule, is the effective nuclear charge and r_A is the Pauling covalent radius], the electronegativities of Ge (2.02) and As (2.20) are higher than those of Si (1.90) and P (2.19).[20] Therefore, it is not surprising that M−O distances are usually shorter in phosphates than in arsenates, as experimentally and computationally confirmed in β-$LiVOXO_4$[48,49] and olivine-$LiCoXO_4$ (X = P, As).[50] Another interesting feature observed in Figure 5 is the different slope of the V^{4+} and V^{5+} guiding lines; the average V−O distance variation in $Li_yV^{5+}XO_5$ is only 0.6% in the entire electronegativity range, in comparison

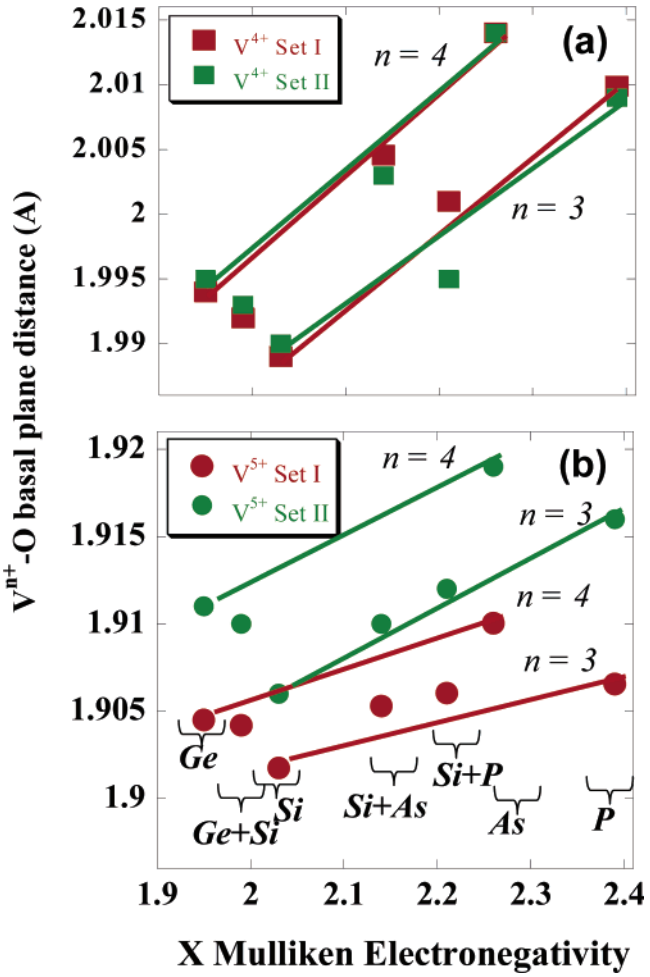

Figure 5. Calculated average V−O(basal) distance as a function of the X electro-negativity in $Li_yV^{4+}OXO_4$ (a) and $Li_{y+1}V^{5+}OXO_4$ compounds (b). Red and green symbols denote data extracted from set I and set II of calculations, respectively. Lines help connect the elements from the same period.

with the 1.2% variation for the lithiated $Li_{y+1}V^{4+}XO_5$ materials. One believes that this effect is rooted in the reduction of the inductive effect from V^{4+} to V^{5+} since V^{5+} renders the V−O bond more covalent. Worth mentioning is that for V^{5+} compounds, although both sets of potentials provide the same general trend, utilizing the more accurate potentials (set II) leads to longer V−O(basal) distances.

The inductive effect of the polyoxyanionic groups is also evident in the vanadyl V═O distances in Figure 6. The evolution of the vanadyl bond with the electronegativity is very similar for V^{4+} (squares) and V^{5+} (circles) series of compounds and independent of the computed set of structures (red, green, and violet symbols denote set I, set II, and the pure-GGA, respectively). Note that as X electronegativity increases, the vanadyl bond shortens. Higher electronegative X elements polarize more effectively the electron density of the V−SP(basal) oxygen, thereby enhancing the polarization

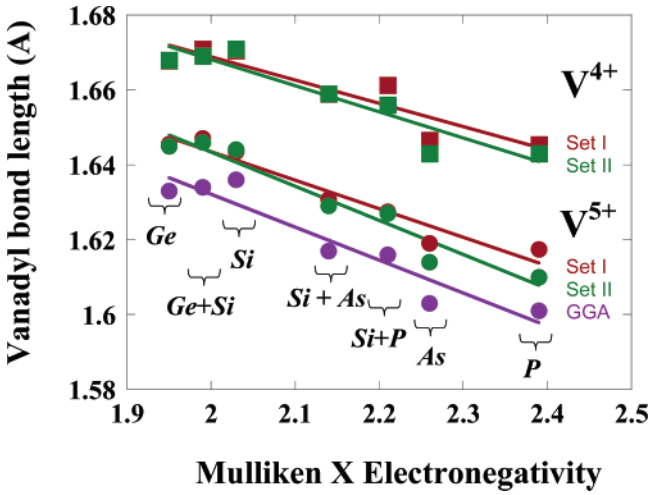

Figure 6. Calculated vanadyl bond length as a function of the X electronegativity in $Li_yV^{5+}OXO_4$ (circles) and $Li_{y+1}V^{4+}OXO_4$ compounds (squares). Red, green, and purple symbols denote data extracted from set I, set II, and pure GGA calculations, respectively. Lines correspond to linear fits.

power of the central V^{5+} (V^{4+}) ion and resulting in a shorter vanadyl bond. The shift between the 3 and 4 periods is less noticeable in the V−O(vanadyl) bond length evolution as compared to the V−O(basal) bond length evolution (Figure 5), which is not surprising since the oxygen atoms in the basal plane are bonded to the X atom while the vanadyl oxygen is not.

In short, considering the structural evolution, one can say that the inductive effect of the polyanionic groups together with the V valence state govern the V−O distances while the overall structure distortion (puckering of the layer) is directly related to the lithium/vacancies ordering. The observed V−O distances evolution with the X electronegativity supports the idea that in polyoxyanionic compounds, with X−O−M bonds, the iono-covalent character of the M−O bond is correlated to the tabulated Mulliken X electronegativity.

(c) Electronic Structure. The correlation between band gaps and electronegativity is well-known for binary compounds within the field of optics.[18,19] For a long time, scientists have been guided to the selection of suitable chemical substitutes to tune the optical gap of the III−V(GaAs) or II−VI(CdTe) semiconductors on a electronegativity−band gap relation. However, not too much is known about whether such a type of relation exists for ternary compounds, making it appealing to seek out band gaps and X electronegativity correlations in the $LiVOXO_4$ family.

Experimentally, we have measured the ac conductivity of Li_2VOSiO_4[11] and Li_2VOGeO_4. Since the pellets had high impedance, we were only able to evaluate their conductivity for temperatures greater than 403 K. Plots of $\log(\sigma)$ vs $1000/T$ (Figure 7) gave a linear dependence that allowed us to calculate the activation energy for conduction according to the Arrhenius relation $\log(\sigma T) = \log(\sigma_0) - \Delta E/k_BT$. An activation energy ($\Delta E$) of 0.96 and 0.91 eV was obtained for the Li_2VOSiO_4[11] and Li_2VOGeO_4, respectively. The extrapolated value of the RT conductivity was found to be very low at around 8×10^{-15} S/cm (assuming that no break in the dependence occurs at lower temperature). Such large room-temperature resistance, together with the large activa-

(48) Gaubicher, J.; Orsini, F.; Le Mercier, T.; Llorente, S.; Villesuzanne, A.; Angenault, J.; Quarton, M. *J. Solid State Chem.* **2000**, *150* (2), 250.
(49) Launay, M.; Boucher, F.; Gressier, P.; Ouvrard, G. *J. Solid State Chem.* **2003**, *176* (2), 556.
(50) Arroyo-de Dompablo, M. E.; Alvarez, M.; Gallardo, J. M.; Amador, U.; Garcia-Alvarado, F. *Solid State Ionics* **2006**, *177* (26−32), 2625−2628.

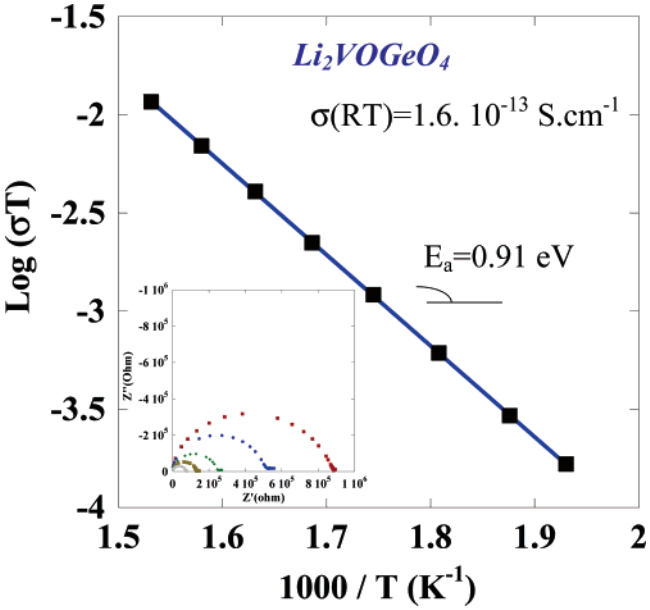

Figure 7. Temperature-dependent conductivity plots for $Li_2VO(Si/Ge)O_4$ pellets. The open symbols are experimental data and solid lines through the open symbols are fit to Arrhenius equation.

tion energy, is consistent with the poor electrochemical performance of these electrode materials in terms of rate capabilities as previously described. No impedance measurements could be performed on the delithiated samples owing to our inability to prepare self-holding pellets.

Information on energy band gaps can be deduced from the calculated density of states. Zhou et al. recently demonstrated that the introduction of a *U* correction term in the GGA method could substantially improve the accuracy of calculated band gaps in highly correlated systems.[51] For instance, in olivine-$LiFePO_4$ the predicted band gap within the GGA+U is 3.8 eV, in good agreement with the measured optical band gap of 3.7−4.0 eV.[51] Even if some reservations still exist about the quantitative prediction of band gaps, it is generally assumed that the general trends extracted from DFT calculations are fully reliable. Figure 8 shows the calculated total density of states (DOS) of $LiVOSiO_4$ (left) and Li_2VOSiO_4 (right), together with the partial DOS of vanadium (green line), basal-oxygen (red line), and vanadyl-oxygen (blue line). In these compounds V ions are in a square pyramid environment, which can be considered as a distorted octahedron with a short V−O bond (vanadyl bond) and a long V−O bond along the *z*-axis. The vanadium $3d_{z^2}$ and $3d_{x^2-y^2}$ orbitals point along the metal−oxygen bond direction, toward the p_x, p_y, and p_z orbitals of the oxygen atoms. This σ overlap results in the bonding σ band, which appears below the Fermi level (predominantly oxygen 2p in character), and the σ^* band above the Fermi level (mostly consisting of vanadium 3d states). In Figure 8 there is a significant mixing of O 2p states and V 3d states in both the σ and σ^* bands, which supplies the direct evidence for the strong covalent interaction of V−O bonds. The vanadium $3d_{xy}$, d_{xz}, and d_{yz} orbitals point in a direction perpendicular to the metal−oxygen bond, being involved in π interactions with the filled oxygen p orbitals of the correct symmetry. This hybridization originates in the octahedral-like t_{2g} bands; the bonding t_{2g} bands appear in the valence band dominated by oxygen 2p states and the antibonding t_{2g} states above the Fermi level. Due to the off-centering of the vanadium atoms from the base of the square pyramid, t_{2g}* splits into two sets of bands; the upper $3d_{yz}/d_{xz}$ one doubly degenerated and the $3d_{xy}$ bottom one. As observed in Figure 8, in $LiVOSiO_4$ the Fermi level resides at the top of the valence band mainly composed of O 2p states, while the conduction band is mostly composed of V $3d_{xy}$ states. Under lithium insertion, diamagnetic V^{5+} is reduced into paramagnetic V^{4+} (d^1 ion); therefore, the DOS of Li_2VOSiO_4 shows majority spin (up spin) and minority spin (down spin) contributions. As observed in Figure 8, in Li_2VOSiO_4 the band gap is the energy difference between the filled up-(V $3d_{xy}$) band (which merges with the O p band) and the empty up-(V $3d_{xz}/d_{yz}$) band.

Figure 9 shows the evolution of the calculated band gaps extracted from set I (red) and set II (green) calculated DOSs as a function of the Mulliken X electronegativity. For reason of completeness we calculated the DOS of V^{5+} compounds within the pure GGA ($U = 0$) approximation (violet points in Figure 9b). All the compounds under study are insulators with calculated band gaps in the range 1.4−2.5 eV. Worth mentioning experimental and calculated data for V^{4+} compounds follow the same general trend with the Mulliken X electronegativity: the gap increases with the electronegativity. In contrast, in Figure 9b it can be seen that for the V^{5+} compounds the band gap decreases with increasing Mulliken electronegativity, displaying an almost linear dependence independent of the set of calculations (set I, set II, or pure GGA).

As mentioned above, the *U* correction term should have a physical meaning. *U* acts as a band gap opener; a larger *U* value leads to a wider energy gap (compare GGA and set I data in Figure 9). In the end, using a too large *U* value in the calculation would result in a significant overestimation of the band gap. Optical measurements are underway to determine the optical band gap of Li_2VOSiO_4. At present, we can confront the calculated data with the measurement activation energies and with the color of the prepared compounds. Calculated gaps (set II) for Li_2VOSiO_4 and Li_2VOGeO_4 are 2.32 and 2.25 eV, respectively; *assuming a semiconductor intrinsic conductivity type*, the activation energy should be half of the band gap, i.e., 1.16 eV for Li_2VOSiO_4 and 1.13 eV for Li_2VOGeO_4. In a very rough approximation these values could be compared with the experimental ones of 0.96 and 0.91 eV (blue points in Figure 9a), even though such a fast comparison is subjected to clarification of which mechanism of electrical conductivity predominates in these compounds. For instance, in olivine-$LiFePO_4$, owing to a localized polaronic-type conductivity, the band gap extracted from the measured temperature dependence of the conductivity (1.95 eV = 2 × E_a) is much smaller than the calculated gap (3.8 eV).[51,52] In the present case, experimental activation energies are of the same order of magnitude as that expected from the calculated gap. Under the picture of *a semiconductor intrinsic conductivity type* this corroborates that our *U* value of 3 eV (extracted form

(51) Zhou, F.; Kang, K. S.; Maxisch, T.; Ceder, G.; Morgan, D. *Solid State Commun.* **2004**, *132* (3−4), 181.

(52) Maxisch, T.; Zhou, F.; Ceder, G. *Phys. Rev. B* **2006**, *73*, 104301.

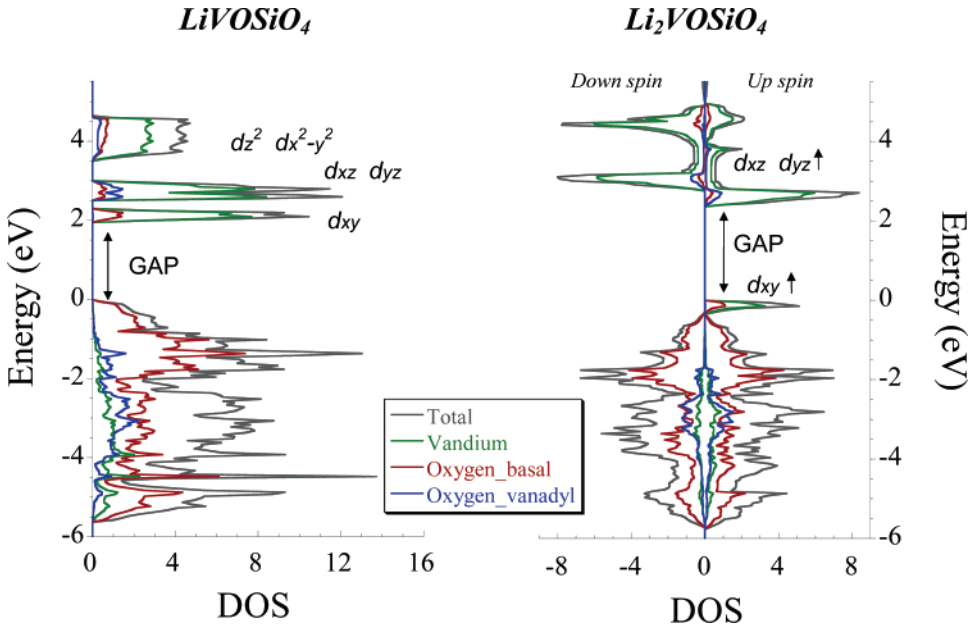

Figure 8. Density of states (DOS) of $LiV^{5+}OSiO_4$ and $Li_2V^{4+}OSiO_4$ compounds calculated within the set II of potentials ($8 \times 8 \times 10$ *k*-point mesh). The gray lines denote the total DOS; the partial DOS of vanadium, basal-oxygen, and vanadyl-oxygen are represented in green, red, and blue lines, respectively. The Fermi level has been arbitrarily chosen as the origin of the energy.

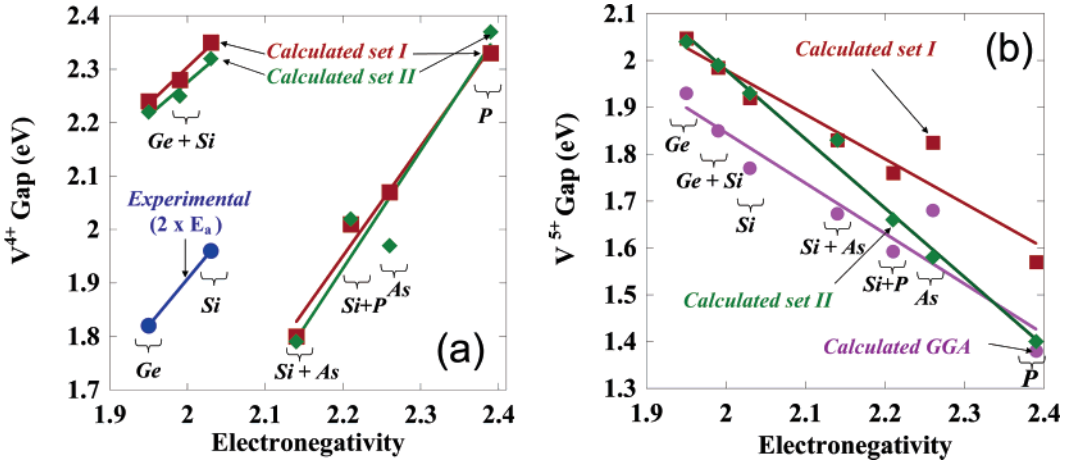

Figure 9. Calculated band gaps for $Li_{y+1}V^{4+}OXO_4$ (a) and $Li_yV^{5+}OXO_4$ (b) as a function of the Mulliken X electronegativity (in Pauling units). Red, green, and purple symbols denote data extracted from set I, set II, and pure GGA calculations, respectively. Experimental data of the activation energy multiplied by 2 are given for comparison. Lines correspond to linear fits.

the lithium insertion potential) is in the correct range. However, quantitatively comparing the "calculated" (1.14 eV) and experimental activation energies (0.93 eV), we cannot discard that this *U* value is somewhat large, therefore resulting in an overprediction of the band gap.

The origin of colors in solids is quite complicated, though, normally, if one knows the color of a compound, one can check if the calculated band structure is in agreement with such a color. The Li_2VOXiO_4 are reddish-brown, and the delithiated $Li_{1.18}VOSiO_4$ form is yellowish-green. In the calculated DOS of $LiVOSiO_4$ (Figure 8 left) there are two possible charge-transfer transitions from the anion band to the V 3d states that fall in the visible spectra. The transition to the V $3d_{xy}$ band is centered at 2.13 eV (absorbed color yellow, observed color blue), and the transition to the V $3d_{xz}$/d_{yz} band is centered at 2.68 eV (absorbed color blue, observed color yellow). Thus, we can expect the color of $LiVOSiO_4$ to be green. According to the calculated DOS of Li_2VOXiO_4 we expect d−d transitions from the filled V $3d_{xy}$ to the unfilled V $3d_{xy}$ centered at 2.57 eV (absorbed color blue-green, observed color orange) and 3 eV (absorbed color violet, observed color green-yellow). This is consistent with the brown coloration of the prepared sample, though a deeper red coloration would require the displacement of the band centered at 2.57 eV to lower energies. This also suggests that though $U = 3$ eV is in the correct range, it might be somewhat large.

It is important to recall that quantitative results in the GGA+*U* method are known to be dependent on the value of the *U* parameter.[33,40,43,52] Overall, it is worth mentioning that DOS calculations are quite useful for giving band gap trends; therefore, caution has to be exercised in literally comparing such DOS calculations on the same compound obtained from different computational approaches (set I and set II in the present work or the Li_2VOSiO_4's DOS in ref 53). Note that in Figure 9 the obtained gaps from set I, set

II, and the GGA are different, but the variation is identical, confirming our statement that solely relative trends and not absolute values have some meaning.

The opposite general trends observed in band gaps of lithiated and delithiated phases can be rationalized from the DOS (Figure 8) attending to the V−O $d_{xy}p\pi$ and V−O (d_{xz}/d_{yz})$p\pi$ overlapping. In the $LiVOSiO_4$ DOS, the V $3d_{xy}$ states hybridize solely with the basal-oxygen states; therefore, the energy of the resulting band depends on the iono-covalent character of the V−O(basal) bonds. A more ionic V−O(basal) bond reduces the overlap between V $3d_{xy}$ and O(basal) 2p orbitals, moving the valence O p band (bonding states) to higher energies and the conduction band (antibonding states) to lower energies. The final result is that the gap between the valence and conduction band gets narrower as the ionicity of the V−O(basal) bond increases. Figure 5 already showed that the V−O(basal) bond is more ionic with the stronger inductive effect of the XO_4 polyoxyanionic group, i.e., higher X electronegativity. On the other hand, the DOS on Figure 8 indicates that the V $3d_{xz}/d_{yz}$ states fully hybridize with the vanadyl-oxygen, and to a lesser extent with the basal-oxygen atoms. The shorter the vanadyl bond (more covalent), the higher the antibonding V $3d_{xz}/d_{yz}$ bands are in energy. In a rough approximation, this energy difference is related to the electronic band gap of V^{4+} compounds (see Figure 8). Therefore, in V^{4+} compounds one can expect the band gap to increase with the X electronegativity parallel to the shorter vanadyl bond length (Figure 6). This general trend is observed in Figure 8a, though there is a shift between the undistorted $Li_2V^{4+}OXO_4$ (X = Si/Ge) and the other compounds, likely rooted in the full lithium site occupancy occurring in the former.

Conclusions

The inductive effect has long been used by solid-state chemists as an intuitive tool to tune the iono-covalency of an M−X bond. In polyoxyanionic structures possessing M−O−X bonds, the *inductive effect* is the polarization of the V−O chemical bond caused by the polarization of the adjacent X−O bond. In this work, we combine experiments and first-principle calculations to investigate whether structural, electronic, and electrochemical properties of the $Li_yV^{5+}OXO_4/Li_{y+1}V^{4+}OXO_4$ (X = P, As, $P_{0.5}Si_{0.5}$, $As_{0.5}Si_{0.5}$, Si, Ge, $Si_{0.5}Ge_{0.5}$) family of compounds correlate to tabulated values of the Mulliken X electronegativity. Computational results evidence that the evolution of both V(4+)−O and V(5+)−O calculated bond lengths correlate to the Mulliken X electronegativity. Calculated electronic band gaps also show a linear correlation to tabulated Mulliken electronegativities; while this is a well-known feature in semiconducting binary compounds, the results presented here provide one of the scarce examples of such relationship in ternary compounds. Furthermore, the computational results predict an almost linear dependence of the lithium insertion voltage of $Li_yV^{5+}OXO_4$ with the Mulliken X electronegativity. Electrochemical experiments carried out on the $Li_2VO(Si/Ge)O_4$ compounds support the computational findings. It should be stressed that the general trends observed are independent of computational parameters as the Hubbard-like correction term (U in the DFT+U) or the basis set utilized in the calculation.

To study the evolution of properties with the X electronegativity in the $Li_yV^{5+}OXO_4/Li_{y+1}V^{4+}OXO_4$ compounds, one should also account for the effect of the different Li site occupancy, y ($1 < y < 2$ for V^{4+} and $0 < y < 1$ for V^{5+}). The capability of first-principles methods to study perfectly ordered structures allowed the deconvolution of the role played by the inductive effect (X electronegativity) and the Li ordering. We found that the lithium content (y) and the lithium/vacancy ordering in the interlayer space drive the structural distortions, while the redox potentials are controlled by the inductive effect. This in accordance with previous experimental observations on the electrochemical behavior of the hexagonal $M_2(XO_4)_3$ hosts,[54] where it was found that the redox energies of the various M cations are nearly independent of the Li ion concentration and distribution over the two types of interstitial sites.

Overall, both experimental and computational techniques show that the V^{4+}/V^{5+} redox potential in Li_yVOXO_4 (X = Si, $Ge_{0.5}Si_{0.5}$, Ge, $Si_{0.5}As_{0.5}$, $Si_{0.5}P_{0.5}$, As, P) is remarkably correlated to values of tabulated Mulliken X electronegativities, making this approach to estimate lithium insertion voltages predictive on a simple basis. As demonstrated by Goodenough in 1997,[6,8,9] using simple iono-covalency considerations linked to electronegativity values, chemists can certainly reach the same trends, but by no means potential redox voltage value ranges. The observed correlation of crystalline, electronic, and electrochemical parameters with the Mulliken X electronegativity leads to the idea of "data transferability" within polyoxyanionic compounds within a given structural type and for a particular redox couple. In light of the "data transferability" concept, the development of novel silicates could make a useful utilization of the wide information available on phosphates, thus minimizing the experimental efforts.

Acknowledgment. This work was supported by the Universidad Complutense de Madrid (PR1/07-14911). M.E.A.D. acknowledges the Spanish MEC for a "Ramon y Cajal" contract. Valuable comments from M. Armand, U. Amador, F. Boucher, M. J. Torralvo, T. Maxisch, E. Moran, J. A. Campo, D. Morgan, A. Vegas, and G. Ceder are greatly appreciated. The authors are grateful to K. Persson for carefully reading the manuscript. Calculations were performed at the CIEMAT supercomputing centre.

CM0612696

(53) Rosner, H.; Singh, R. R. P.; Zheng, W. H.; Oitmaa, J.; Pickett, W. E. *Phys. Rev. B* **2003**, *67* (1), 014416.

(54) Padhi, A. K.; Manivannan, O. V.; Goodenough, J. B. *J. Electrochem. Soc.* **1998**, *145* (5), 1518..

(55) Shannon, R. D.; Prewitt, C. T. *Acta Crystallogr.* **1969**, *B25*, 925.

(56) Jordan, B.; Calvo, C. *Can. J. Chem.-Rev. Can. Chim.* **1973**, *51* (16), 2621.